AIAA JOURNAL
Vol. 42, No. 3, March 2004

Investigation of Helicopter Rotor-Blade-Tip-Vortex Alleviation Using a Slotted Tip

Yong Oun Han*
Yeungnam University, Gyongsan 712-749, Republic of Korea
and
J. Gordon Leishman†
University of Maryland, College Park, Maryland 20742

A slotted tip was developed to modify the characteristics of the strong vortex trailed from the tip of a small-scale helicopter blade. Forward-facing slots directed a slight amount of the incident flow in the spanwise direction, which was vented at the side edge of the blade tip. This caused the tip vortex to detach from the blade tip face, and also introduced turbulent vortlets into the laminar core of the developing vortex. The resulting wake flowfield was investigated using flow visualization and laser Doppler velocimetry. Measurements were conducted to quantify the vortex swirl velocity components, the inner core development, and the overall vortical flow inside the vortex trails. The results were then compared to a baseline blade with a standard unmodified rectangular tip. It was found that the slotted blade reduced the peak value of the swirl velocity components in the tip vortex by up to 60% relative to those of the baseline blade. The core growth of the tip vortices from the slotted blade suggested a much higher rate of diffusion, up to as much as three times that of the baseline case. Measurements of rotor power showed only a 3% increase relative to the baseline tip. Based on the overall results, the slotted blade is considered a highly effective design in diffusing vorticity and reducing the flow high field velocities that would otherwise be induced by a rotor tip vortex.

Nomenclature

C_T	=	rotor thrust coefficient, $T/(\rho A\Omega^2 R^2)$
c	=	rotor-blade chord, m
e	=	correlation coefficient
p	=	probability density function
R	=	rotor radius, m
Re_v	=	vortex Reynolds number, Γ/ν
r	=	radial distance, m
$\bar{r}$	=	nondimensional core radius, r/r_c
r_c	=	viscous core radius, m
r_p, z_p	=	laser Doppler velocimetry measurement location with respect to rotor axes
r_v, z_v	=	vortex core location with respect to rotor axes
r_0	=	initial core radius, m
T	=	rotor thrust, N
t	=	time, s
V	=	velocity, ms^{-1}
V_θ	=	swirl velocity, ms^{-1}
α	=	Oseen constant, 1.25643
Γ	=	circulation, $\mathrm{m}^2\mathrm{s}^{-1}$
Γ_c	=	core circulation, $\mathrm{m}^2\mathrm{s}^{-1}$
δ	=	effective diffusion constant
ζ	=	wake (vortex) age, deg
ν	=	kinematic viscosity, $\mathrm{m}^2\mathrm{s}^{-1}$
ρ	=	flow density, $\mathrm{kg\ m}^{-3}$
σ_r, σ_z	=	standard deviation of vortex location in radial and axial directions, respectively, m
Ω	=	rotor rotational speed, $\mathrm{rad\ s}^{-1}$

Received 19 June 2003; revision received 26 September 2003; accepted for publication 20 October 2003.

*Professor, School of Mechanical Engineering; yohan@yu.ac.kr.
†Professor, Department of Aerospace Engineering, Glenn L. Martin Institute of Technology; leishman@eng.umd.edu.

Introduction

DURING the past two decades, considerable research has been conducted into the problem of measuring and understanding the development of the blade tip vortices trailed into the wakes of helicopter rotors. The motivation for this is clear, in that the structure of the tip vortices defines a majority of the induced velocity field surrounding the rotorcraft.[1,2] The strong, concentrated tip vortices generated by a helicopter rotor blade (or by the proprotors on a tilt rotor) can also be a source of adverse aerodynamic problems, such as blade vortex interactions (BVI) and vortex–airframe interactions. In each case, it is the high induced velocities surrounding the tip vortices that become a source of unsteady aerodynamic forces, and these can be a significant source of rotor noise and airframe vibrations. In particular, it is known that small changes in the structure of the tip vortices and their positions relative to the rotor blades can have substantial effects on BVI noise (e.g., Ref. 3). The reduction of rotor noise has become an extremely important goal in the design of military and civil rotorcraft.

In principle, it is plausible to modify the structure of the tip vortices by diffusing their concentrated vorticity, which can significantly reduce or even eliminate the forenamed adverse aerodynamic problems. However, the goal of producing the rapid and effective diffusion of vorticity inside tip vortices is not a new approach, nor is it a easy one to meet. Various approaches have been considered, such as with the use of various types of tip shape modifications[4–6] including subwings[7,8] or spoilers.[9] Active flow control and passive flow control have also been suggested for this purpose.[10,11] These techniques all basically act to modify the tip vortex structure in some way, or perhaps change its stability characteristics. Yet, the reduction of the induced velocity field surrounding the tip vortex has been found to be difficult to accomplish without incurring some other form of rotor performance penalty, which usually appears as an increase in profile power at the rotor.[5] Actively controlled devices also require some additional power[11] to establish the blowing/suction or unsteady excitation of the boundary layers at the blade tip, and also require additional nonstructural mass for the flow control mechanism(s). Therefore, the ideal goal for tip vortex alleviation is to use some form of simple, lightweight, low-cost passive flow-control device, and also to strive for a device that incurs little or no other adverse effects on overall rotor performance.

Toward this goal, a slotted blade tip has been suggested in recent experiments,[12,13] and very encouraging initial results have been obtained. The first experiments using the slotted tip were carried out by using both a fixed wing and a rotating blade. The slotted wing and slotted tip blade were made by imbedding flow slots or channels inside the tip region, but without any change of the external tip geometry or surface shape. These slots create a pressure gradient between the entrance and exit, which allow a slight amount of the incident flow to pass through the tip in the spanwise direction and exit the side edge of the blade. This was found to diffuse more rapidly the concentrated vorticity within the tip vortex.[12,13]

This paper describes new results that were measured using a improved slotted rotor-tip geometry on a model rotor blade operating in the hover state. Narrow tube diameter slots compared to the blade thickness were used. The inlet to the slot array was also moved more toward the upper surface of the blade, which based in the results from previous work[12,13] was a first step toward optimizing the effectiveness of the slot locations. Extensive flow visualization was carried out to study the resulting vortical flow structures. Phase-resolved measurements of the vortex flow structure were also made using three-component laser Doppler velocimetry (LDV).

Description of the Experiment

Rotor Facility

A single-bladed rotor operated in the hovering state was used for the measurements. The advantages of the single-blade rotor have been addressed before.[14,15] This includes the ability to create and study a helicoidal vortex filament without interference from other vortices generated by other blades,[14] thereby allowing the aerodynamic effects of the tip shape itself to be more clearly delineated. Also, a single helicoidal vortex is much more spatially and temporally stable than with multiple vortices,[15] thereby allowing the tip vortex structure to be studied to much older wake ages and also free of the high aperiodicity issues in the flow that usually plague multibladed helicopter rotor experiments.

The rotor was tested in the hovering state in a flow-conditioned test cell. The volume of the test cell was approximately 362 m^3 (12,800 ft^3) and was surrounded by honeycomb flow-conditioning screens. This cell was located inside a large 14,000 m^3 (500,000 ft^3) high-bay laboratory. The rotor wake was allowed to exhaust approximately 18 rotor radii before encountering flow diverters. Aperiodicity levels in the rotor wake were measured using flow visualization, and the aperiodicity statistics were used to correct the velocity field measurements (see Appendix).

Blade Design

The single blade was of rectangular planform, untwisted, with a radius of 406 mm (15.98 in.) and chord of 44.5 mm (1.752 in.) and was balanced with a counterweight. The blade airfoil section used was the NACA 2415, which was constant throughout the blade.

The slot system, which was composed of internal tubes, was imbedded inside the chord plane of the blade at the tip region, as shown in the schematic of Fig. 1. Because of the pressure gradient between the inlet and exit, the slots bypass a slight amount of the incident flow through the tip and turns it in the spanwise direction to be ejected out of the face at the blade tip. While the internal slot system used by Han and Chung[13] was placed exactly on the chord plane, in the present design the slot entrances were located slightly above the chord plane because based on preliminary experiments this seemed to improve the effectiveness of the design. The baseline blade was defined by covering the slot entrances with thin Mylar tape.

In each case, the rotor was operated at a tip speed of 89.28 m/s (292.91 ft/s), giving a tip Mach number and chord Reynolds number of 0.26 and 2.72×10^5, respectively. Most of the tests were made at a thrust coefficient of $C_T \approxeq 0.002$ using a collective pitch of 4.0 deg (measured from the chord line).

Flow Visualization

Flow-visualization images were acquired by seeding the flow using a mineral oil fog strobed with a laser sheet. This light sheet was produced by a dual Nd:YAG laser. The light sheet was located to any location and orientation in the flow using an articulated optical arm. Images were acquired using a high resolution charge-coupled-device (CCD) camera. The laser and the camera were synchronized to the rotor one-per-rev frequency, and a phase delay was introduced so that the laser could be fired at any rotor phase (azimuth) angle.

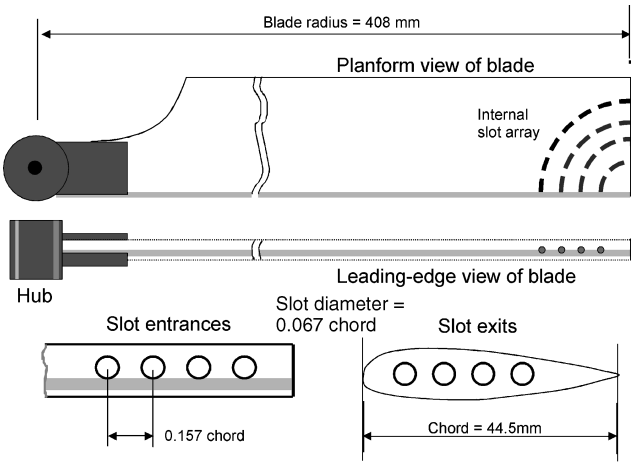

Fig. 1 Schematic of the slotted tip blade.

The seed particles were produced by vaporizing mineral oil into a dense fog. From a calibration, 95% of the particles were between 0.2 and 0.22 μm in diameter. The mean seed particle size was small enough to minimize particle tracking errors for the vortex strengths.[16] The fog/air mixture was passed through a series of ducts and introduced into the rotor flowfield at various strategic locations to give acceptable seeding concentrations for either flow visualization or LDV. The high capacity of the seeder allowed the entire test cell to be uniformly seeded in approximately 30 s.

LDV System

A fiber-optic-based LDV system was used to make three-component velocity field measurements. A beam splitter separated a single 6-W multiline argon-ion laser beam into three pairs of beams (green, blue, and violet), each of which measured a single component of velocity. A Bragg cell, set to a frequency shift of 40 MHz, produced the second shifted beam of each beam pair. The laser beams were passed to the transmitting optics by a set of fiber-optic couplers with single-mode polarization preserving fiber-optic cables. The transmitting optics were located adjacent to the rotor and consisted of a pair of fiber-optic probes with integral receiving optics, one probe for the green and blue pairs and the other probe for the violet pair. Beam expanders with focusing lenses of 750 mm were used to increase the beam crossing angles and so to decrease the effective measurement volume.

To further reduce the effective size of the probe volume visible to the receiving optics, the off-axis backscatter technique was used, which is described by Martin et al.[17] and Barrett and Swales.[18] This technique spatially filters the effective length of the LDV probe volume on all three channels. Spatial coincidence of the three probe volumes (six beams) and two receiving fibers was ensured to within a 15-μm radius using an alignment technique[17] based on a commercially available laser-beam profiler.

Signal bursts from seed particles passing through the measurement volume were received by the optics and transmitted to a set of photomultiplier tubes where they were converted to analog signals. This analog signal was low-band-pass filtered to remove the signal pedestal and any high-frequency noise. The large range of the low-band-pass filter was required to allow measurement of the flow reversal associated with the convection of a vortex core across the measurement grids. The analog signal was digitized and sampled using a digital burst correlator. The flow velocities were then converted into three orthogonal components based on measurements of the beam crossing angles. Each measurement was phase resolved with respect to the rotating blade by using a rotary encoder, which

tagged each data point with a time stamp. The measurements were then phase averaged into 1-deg bins.

Results and Discussion

Flow Visualization

Tip Vortex from the Baseline Blade

The flow-visualization experiments gave considerable insight into the tip-vortex developments and the changes in the filament structure as it was convected through the flow below the rotor. Sequential time images of planes through the vortex core were obtained, the vortices being targeted by the Nd-YAG laser. For the baseline blade, the results for which are shown in Fig. 2, the tip vortex and its inner core region are shown for wake ages of $\zeta = 15$, 60, 90, 145, 180, 270, and 375 deg, respectively. The image at $\zeta = 15$ deg also shows the tip vortex at $\zeta = 375$ deg as well as the shadow of the blade tip, which is just about to leave the illuminated image plane.

As is apparent from Fig. 2, the inner region of the vortex is demarcated as a distinct void of seed particles. This void becomes larger as the vortex ages and occurs because of the centrifugal and Coriolis

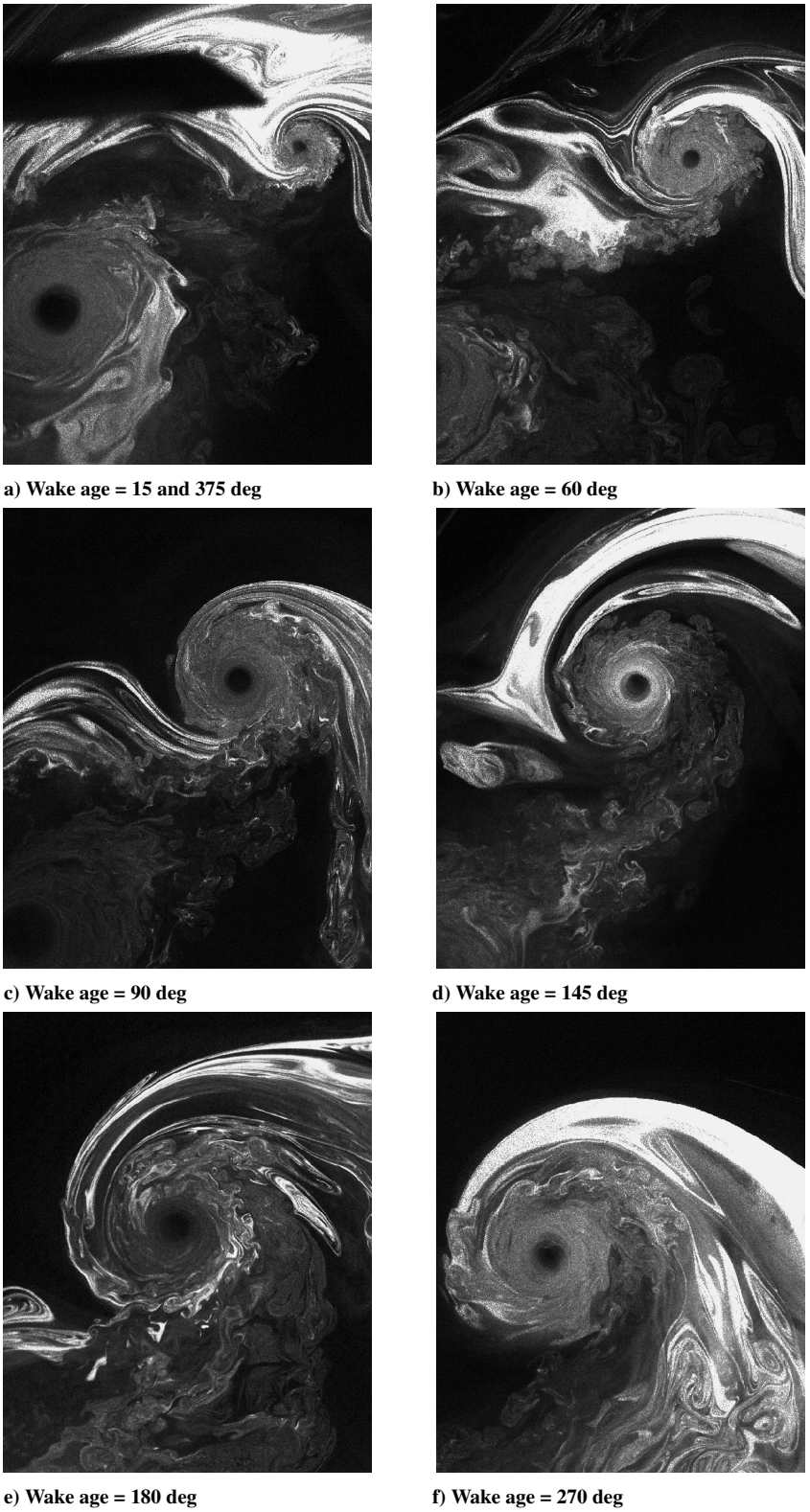

a) Wake age = 15 and 375 deg **b) Wake age = 60 deg**

c) Wake age = 90 deg **d) Wake age = 145 deg**

e) Wake age = 180 deg **f) Wake age = 270 deg**

Fig. 2 Flow visualization of the vortex wake generated by the baseline blade at wake ages of $\zeta = 15$, 60, 90, 145, 180, 270, and 375 deg, respectively.

forces acting on the seed particles by the high particle accelerations near the inner region of the vortex.[16] The flow visualization showed clear features in the resulting vortex structure. The overall flow structure suggested a significant radial partitioning of the vortex development, as can be seen in each of the images in Fig. 2. This radial partitioning is a part of the transitional process.[19] It is well known in fluid dynamics that any flow energy containing a large eddy-like tip vortex must experience equipartitioning (or cascading) into many tiny eddies during its diffusing or decaying process.[20]

Moving out in the radial direction from the center of the vortex, Fig. 2 shows that there first appears smooth circular bands of seed. This suggests a relatively laminar inner region with little or no flow mixing. Here, diffusion of vorticity can occur only at a molecular level, which is extremely slow. Outside of this region, there are many eddies and considerable turbulent mixing clearly occurs here. This mixing contributes to the overall vorticity diffusion mechanism, which helps to more rapidly diffuse the vorticity away from the vortex core. Overall, it can be seen from this set of sequential flow-visualization images that the tip vortex grows from a mostly laminar flow structure at young wake ages to a somewhat more overall diffused and turbulent flow structure as the vortex ages. However, in this baseline case the tip vortex retains its laminar inner core region at all wake ages.

The vortex sheet trailed from the inner part of the blade is connected to the tip vortex. This vortex sheet, which is composed of small-scale turbulent eddies that have their origin from the merging upper and lower boundary layers on the blade, does not have sufficient intensity to substantially influence the development or diffusion of the tip vortex. Furthermore, it is apparent that as these eddies become entrained into the tip vortex they appear to be damped out, and the flow then becomes more laminar. This is why devices that attempt to modify the tip-vortex structure by creating flow disturbances or turbulence outside the core boundary[4–7] are largely ineffective in diffusing vorticity. Further discussion of this point is made later.

Tip Vortex from the Slotted Blade

Flow-visualization results from the slotted blade are shown in Fig. 3, images from which were obtained at comparable wake ages as for the baseline blade. In this case, it was apparent that as the tip vortex forms and rolls up along the tip side edge the exit flow from the slots acts in such a way as to break up the laminar inner region. Therefore, this initial action begins to quickly promote turbulence inside the innermost region of the tip vortex, which would otherwise remain laminar.

As can be seen from the flow-visualization images, in this case there is little evidence of a well-defined laminar inner region. Furthermore, there is no seed void at the core center, which confirms enhanced flow mixing there. Therefore, it is apparent that the slots promote flow mixing inside the tip vortex, and so it can be expected that tip vortex generated by the slotted blade is initially more diffused. By this reasoning, it can also be expected to defuse faster than it does for the baseline case (see quantitative measurements made later). Because the tip vortex generated by the slotted blade has no apparent laminar inner region, even in the early stages after formation, in this case it can also be influenced more easily by action of external effects such as by the entrainment of the vortex sheet or by interactions with adjacent vortices.

To further investigate how the slots function to destroy the inner laminar region of the tip vortex and to enhance turbulent diffusion of vorticity away from the vortex core, close-up flow-visualization images in the blade-tip region were obtained by placing the laser sheet at different orientations and making zoomed-in images from two different observation angles, mainly parallel and perpendicular to the rotor-tip path plane. Representative results are shown in Fig. 4. As can be seen in these images, the four slots in the tip allow a slight amount of flow to pass through the slots, which exit as turbulent jets at the blade tip face. It was found from the flow visualization that small, discrete, turbulent vortlets were formed at each of the slot exits. It is apparent that there are two forms of coherent flow structures in this case. First, there is an overall roll up of the tip vortex just like the baseline blade. Second, an inner bundle of turbulent vortlets are formed, all of which rotate in the same direction. These vortlets then seem to easily roll up around each other and penetrate the inner region of the vortex core. This mechanism acts to dissolve the inner laminar region and promote turbulence. A schematic of the formation process is given in Fig. 5, which has been deduced from several flow-visualization images.

When these turbulent vortlets fill the void of the vortex core, they introduce flow mixing and dissolve the laminar inner region that would otherwise be caused by the strong angular momentum at the beginning of the vortex roll up. Consequently, this process acts to diffuse the vorticity inside the tip vortex much more rapidly than for the baseline tip, even although it is apparent from the flow visualization that the tip vortex still exists in a coherent form. Basically, the tip vortex from the slotted blade still retains the radial partitioning features, but now the effect of the turbulent inner region becomes the dominant process that affects the overall process of diffusing vorticity from the vortex core.

Velocity Field Measurements

The velocity field and net rate of vorticity diffusion of the tip vortex were quantified by LDV measurements. Results for the swirl component of the velocity in the tip vortex at various wake ages are shown in Fig. 6. The results are shown in the form of swirl velocity nondimensionalized by tip speed and distance from the core nondimensionalized by the core radius of the baseline blade (see next). All of the measurements were corrected for the effects of flow aperiodicity, the procedure which is described in the Appendix. The results have also been placed in a reference axis system moving with the convecting flow, so that the measured convection velocity has been removed.

Compared to the measurements made on the baseline blade, it is apparent from Fig. 6 that the peak swirl velocity values induced by the slotted blade were reduced by 20% to as much as 60% at comparable wake ages (see also Tables 1 and 2). This appears to be a somewhat greater reduction in swirl velocity than was found in a preliminary experiment[13] and confirms that the idea of relocating the slot entrances slightly above the chord line is more effective in diffusing the tip-vortex core. The slot entrance on the blade in the preliminary experiment was located closer to the chord line at the leading edge, the initial idea being to maximize the pressure gradients between the slot entrances and exits and so to induce a maximum flow rate through slots. Compared to the present results, however, it is apparent that this does not necessarily result in the most effective reduction in the swirl velocity, and perhaps further work still needs to be done to more precisely optimize the slot locations.

By plotting the swirl velocities nondimensionalized by the peak swirl velocity against the distance from the core nondimensionalized

Table 1 Core radius and peak swirl velocity for the baseline blade

Wake age, deg	r_c/c	$V_{\theta_{\max}}/\Omega R$
3.0	0.016	0.3540
29.0	0.054	0.1339
56.0	0.052	0.1281
144.0	0.066	0.1295
185.0	0.090	0.1225
265.0	0.092	0.1181
362.0	0.120	0.1055
438.0	0.102	0.0903

Table 2 Core radius and peak swirl velocity for the slotted blade

Wake age, deg	r_c/c	$V_{\theta_{\max}}$(slot)/$V_{\theta_{\max}}$(base)
2.0	0.040	0.786
28.0	0.128	0.627
58.0	0.164	0.456
145.0	0.170	0.528
185.0	0.148	0.328

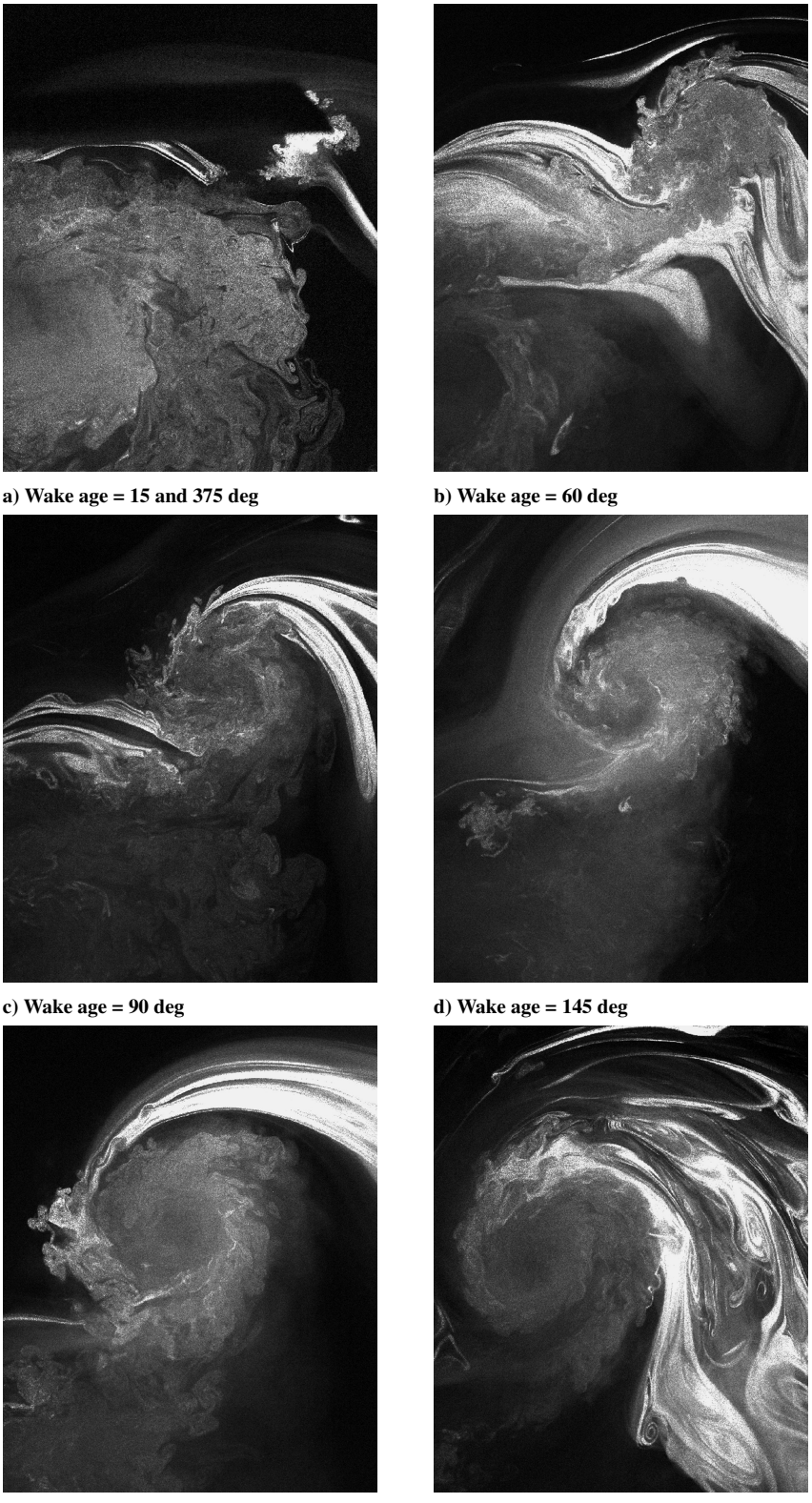

a) Wake age = 15 and 375 deg

b) Wake age = 60 deg

c) Wake age = 90 deg

d) Wake age = 145 deg

e) Wake age = 180 deg

f) Wake age = 270 deg

Fig. 3 Flow visualization of the vortex wake generated by the slotted blade at wake ages of $\zeta = 15$, 60, 90, 145, 180, 270, and 375 deg, respectively.

by the core radius, a series of fairly self-similar profiles were obtained, as shown in Fig. 7. The vortex core radius is nominally half the distance between the peaks in the swirl velocity profile. A more precise and less subjective determination of the core radius was made by fitting a curve to the measurements in a least-squares sense (Fig. 6) and finding the peak velocity and corresponding core size from the curve fit. The results are shown separately for the baseline tip and the slotted tip. In each case, the swirl velocity from a series of desingularized vortex models are shown for reference. At the earliest wake ages ($\zeta \approx 3$ deg) it is apparent that the tip vortex is still in the process of formation and does not follow any of the models. For the later wake ages, the swirl velocity of the slotted blade compares fairly well to the $n = 1$ case of Vatistas's general algebraic model,[21] while those of the baseline blade fit better to the classic Lamb–Oseen model[22,23] or the $n = 2$ case of Vatistas's model. These observations imply that the slotted

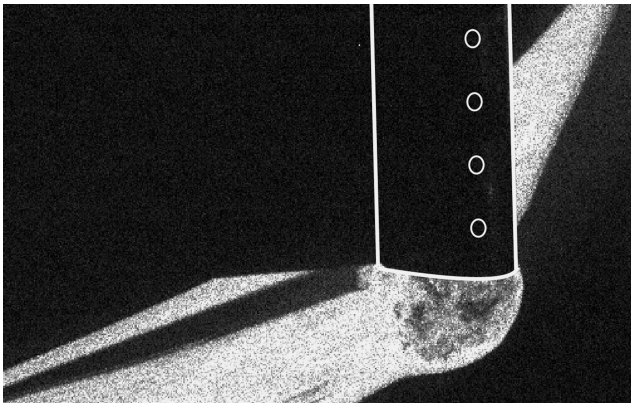

a) View at leading edge of slotted blade

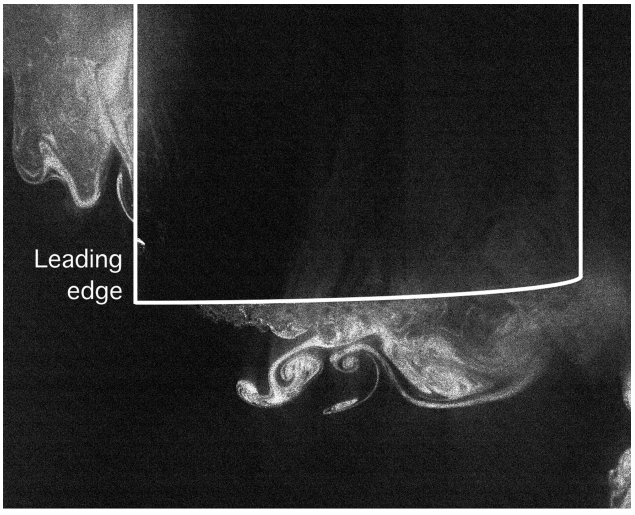

b) View normal to rotor tip-path-plane

Fig. 4 Detailed flow visualization of the region near the tip of the slotted blade: a) looking at the leading edge with the laser sheet perpendicular to the rotor plane and b) looking down on the rotor nearly perpendicular to the tip path plane; flow is from left to right.

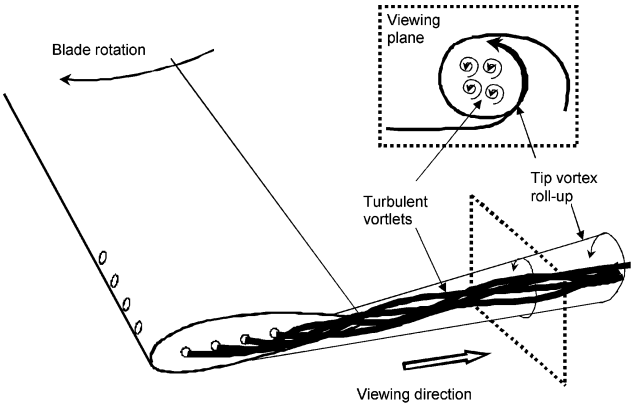

Fig. 5 Schematic showing the process of dissolving the laminar inner region of the tip vortex by the action of turbulent vortlets generated at the slot exits.

blade generates somewhat milder velocity gradients within the core region, which is a direct manifestation of the production of the turbulent vortlets and small eddies during the initial stages of tip-vortex formation.

Core Developments

Compared to measurements made on a previous baseline blade,[6] the present measurements suggest a slightly larger inner core size, as shown in Fig. 8. The only difference between the present baseline blade and the prior blade was that the exits of the slot at the tip face were left open. This can have had some effect on the initial vortex core development because it can be expected that there must be boundary-layer effects on the side edge of the blade tip. As shown in Fig. 8 and in Tables 1 and 2, the results indicated that the tip-vortex core sizes for the slotted blade tip were between 1.6 to 3.1 times larger than for the baseline blade when compared at equivalent wake ages.

Although a variety of mathematical models have been suggested to describe the diffusion of vortices, one of the simplest is the classic Lamb–Oseen model.[22,23] However, the spin down of the swirl velocity and core growth given by the Lamb–Oseen model is found to be unrealistically slow when compared to measurements. This is because of the laminar flow assumptions invoked in the model, that is, only molecular diffusion throughout the vortex is allowed.

In light of consolidated experimental evidence,[24] empirically modified Lamb–Oseen growth models are found to give better representations of the velocity fields surrounding rotor tip vortices. Bhagwat and Leishman[24,25] have modified the Squire model[26] with the inclusion of an average apparent viscosity parameter δ to account for turbulence mixing on the net rate of diffusion, effectively increasing the core growth rates to values that are more consistent with experimental observations. The core radius r_c of the tip vortices can then be effectively modeled as a function of age ζ, using the equation

$$r_c(\zeta) = \sqrt{4\alpha\delta\nu[(\zeta - \zeta_0)/\Omega]} \equiv \sqrt{r_0^2 + 4\alpha\delta\nu\zeta/\Omega} \qquad (1)$$

If $\delta = 1$, then the Lamb–Oseen result is obtained. The ordinate shift ζ_0 is responsible for the nonzero effective core radius r_0 at the tip-vortex origin (where $\zeta = 0$ deg), to give a more physically correct (finite) induced velocity there compared to the Lamb–Oseen result. The results in Fig. 8 suggest that a value of $\delta = 8$ is appropriate for the baseline tip case, whereas the slotted blade tip, on average, suggests considerably higher effective values.

To better appreciate the increase in the core size and change in the vortex core structure obtained with the slotted blade, the measured core dimension is superimposed on a close-up flow-visualization image at three different wake ages, as shown in Fig. 9. Results are shown for both the baseline and slotted blades at approximately the same wake age. It is clear that the slotted blade has caused the core dimension to grow significantly compared to the baseline case. As mentioned earlier, the introduction of the turbulent eddies from the slot exits encourages turbulent mixing within the otherwise laminar vortex core, and a more rapid radial diffusion of vorticity is produced. This mechanism causes the vortex core to grow much more rapidly as the vortex ages in the flow.

Richardson Number

Cotel and Bridenthal[27] and Cotel[28] have made a study of tip vortices trailed by fixed wings and suggested that the diffusion of vorticity in the vortex core is dominated by laminar flow effects. These authors work on the assumption that the high rotational velocities cause stratification inside the vortex core[29] and use a Richardson number to explain their concept. The attainment of a critical value of the Richardson number, which is a function of vortex Reynolds number, suggests that the rotational velocity can become high enough to prevent the development of turbulence within that region of the vortex. This model is interesting because it helps to explain some features seen in the present work.

The local Richardson number is defined as

$$Ri = \frac{2V_\theta}{r^2}\frac{\partial(V_\theta r)}{\partial r} \Bigg/ \left[r\frac{\partial(V_\theta/r)}{\partial r}\right]^2 \qquad (2)$$

From the measured swirl velocity profiles, the corresponding distribution of the local Richardson number can be calculated,

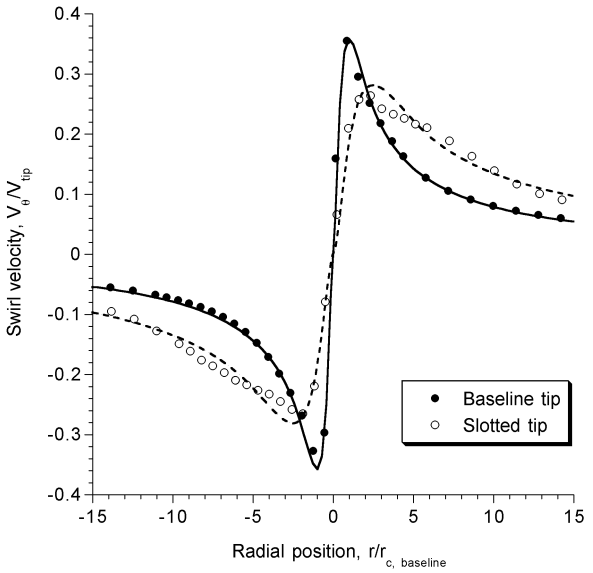

a) Wake age = 3 deg

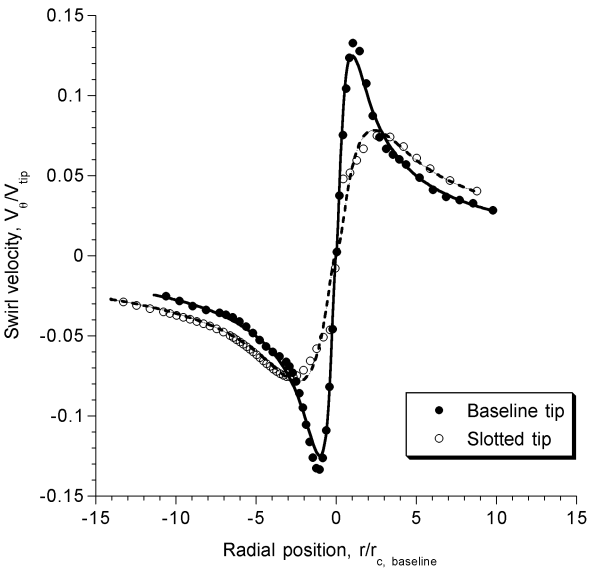

b) Wake age = 29 deg

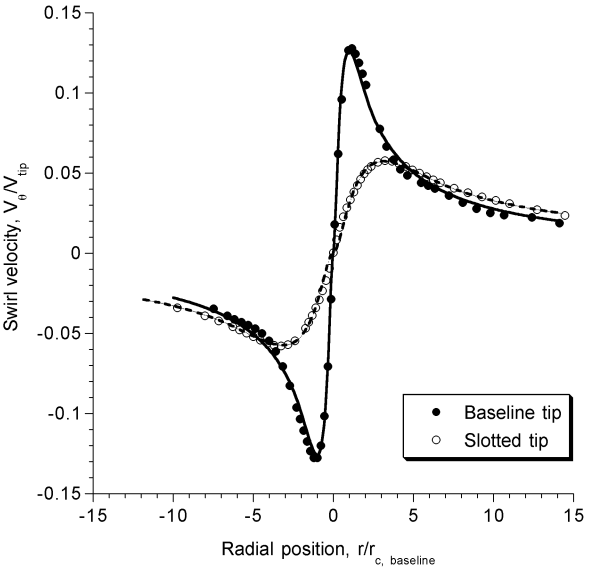

c) Wake age = 56 deg

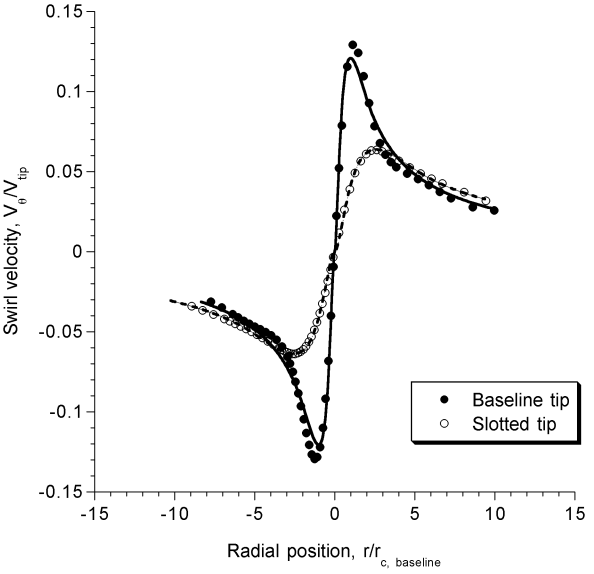

d) Wake age = 144 deg

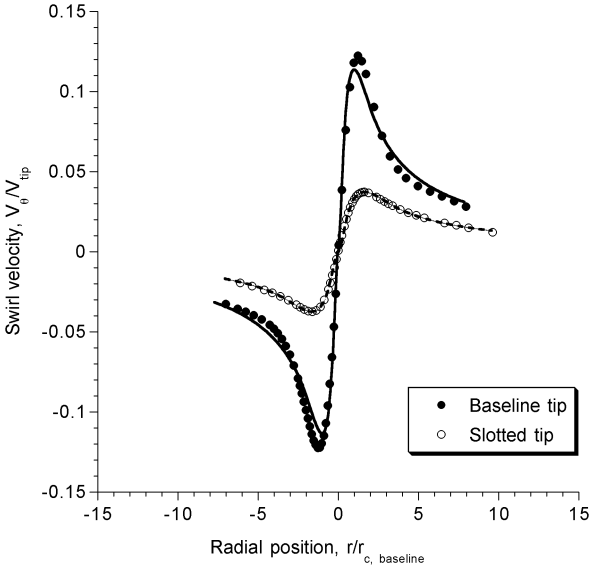

e) Wake age = 185 deg

Fig. 6 Comparison of swirl velocities of both blade at their comparable wake ages with best curve fits (——, for the baseline blade and – – –, slotted blade).

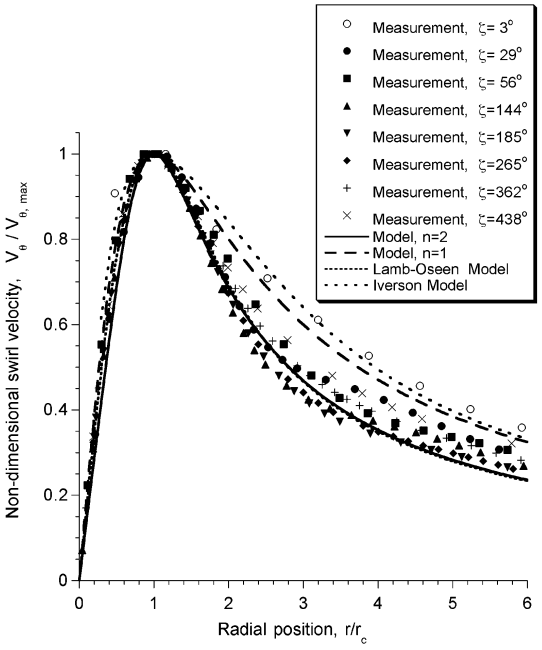

a) Baseline tip

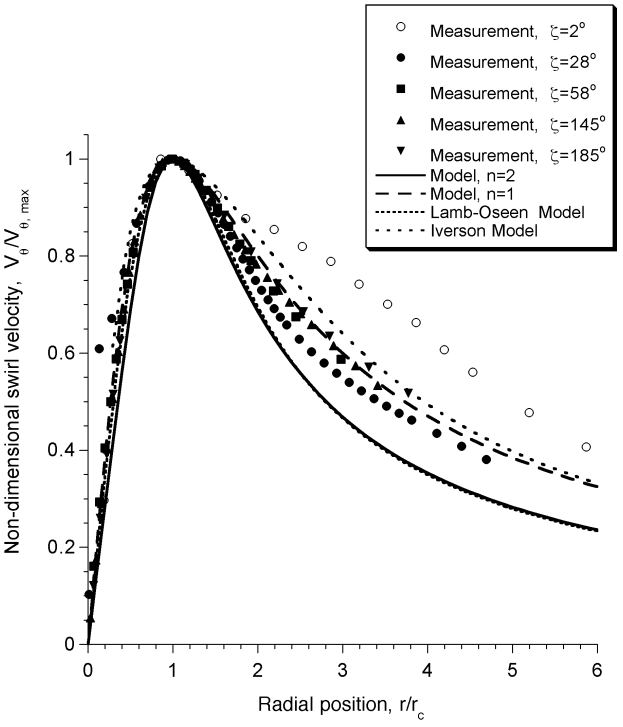

b) Slotted tip

Fig. 7 Normalized swirl velocity components.

which is plotted in Fig. 10 for both blade tips. The critical Richardson number[27,28] is given in terms of the vortex Reynolds number as

$$Ri(\text{critical}) = Re_v^{\frac{1}{4}} \tag{3}$$

It is hypothesized that the attainment of the critical Richardson number will prevent the formation of turbulent eddies or relaminarize any entrained eddies, and so will allow diffusion to take place in this region only by the relatively slow process of molecular diffusion.

Notice that Eq. (2) requires the evaluation of the radial gradient of the swirl velocity profiles, and so care must be taken in determining the slope of the velocity profile near the core radius where its rate of change is high. There is not much difference in the Richardson-

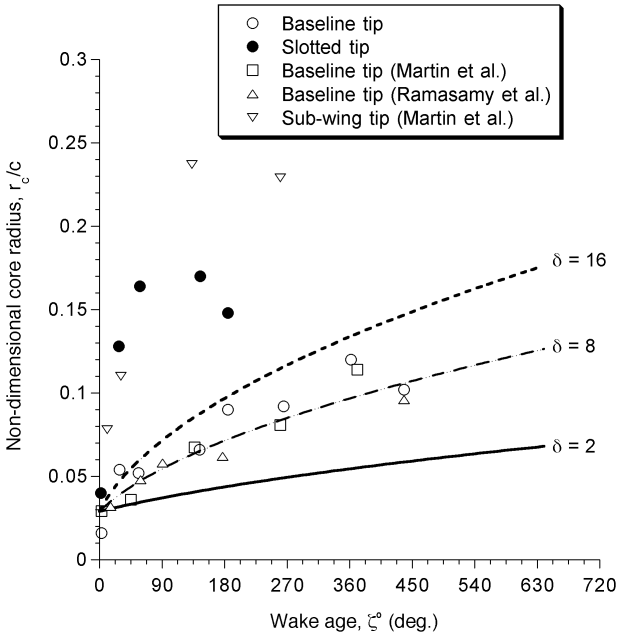

Fig. 8 Growth in the vortex core radius (inferred from velocity profiles) as a function of wake age.

number results between both blade tips, as shown in Fig. 10. Yet compared to the baseline tip case, which fits well to the fully laminar Lamb–Oseen model, the tip vortex of the slotted blade tends to have values of the Richardson number that suggest a more turbulent vortex structure overall, mainly because it follows the result based on the fully turbulent Iversen profile.[30] This is consistent with the flow-visualization results, as discussed earlier.

Based on the foregoing observations, it is apparent that the high rotational velocities will allow stratification of the flow around the vortex core boundary even for the slotted blade. It means that during the partitioning process the small eddies that can develop and surround the core boundary cannot progress into the core region. This implies that the vortex will defuse relatively slowly. Furthermore, this process can be affected by the adjacent interference of another part of the vortex spiral, which can interchange fluid.[2] It is also clear that the turbulent vortlets produced at the face of the slotted blade cannot immediately pass out of the core region but instead act to make the core region homogenously turbulent and promote the more rapid growth of the core. Because the laminar core center of the vortex has a low value of static pressure, the laminar vortex allows the vortlets generated by the slots to enter the core region rather willingly. It is, therefore, apparent then that the slotted blade design is a most effective device in diffusing the vorticity in the vortex and so reducing its peak swirl velocities.

Vortex Circulation

The vortex circulation can be estimated from the measured swirl velocity distributions given earlier using the following axisymmetric flow definition:

$$\Gamma/\Omega Rc = 2\pi(V_\theta/\Omega R)(r/c) \tag{4}$$

The results are shown in Fig. 11. In the case of the baseline tip at the earliest wake age, the tip vortex is still in the process of formation and has not attained its full strength. At later wake ages, it is apparent that there is some scatter in the values of circulation. This is not unexpected as it is well known that the far-field value of tip vortex strength in a helicopter rotor wake is difficult to measure because it is difficult to exclude extraneous circulation in other parts of the flowfield such as the vortex sheet.[31] Because the vortex generated by the slotted blade has a more diffused and radially expanded core region, it was even more difficult to obtain the net value of the induced circulation at large radial distances.

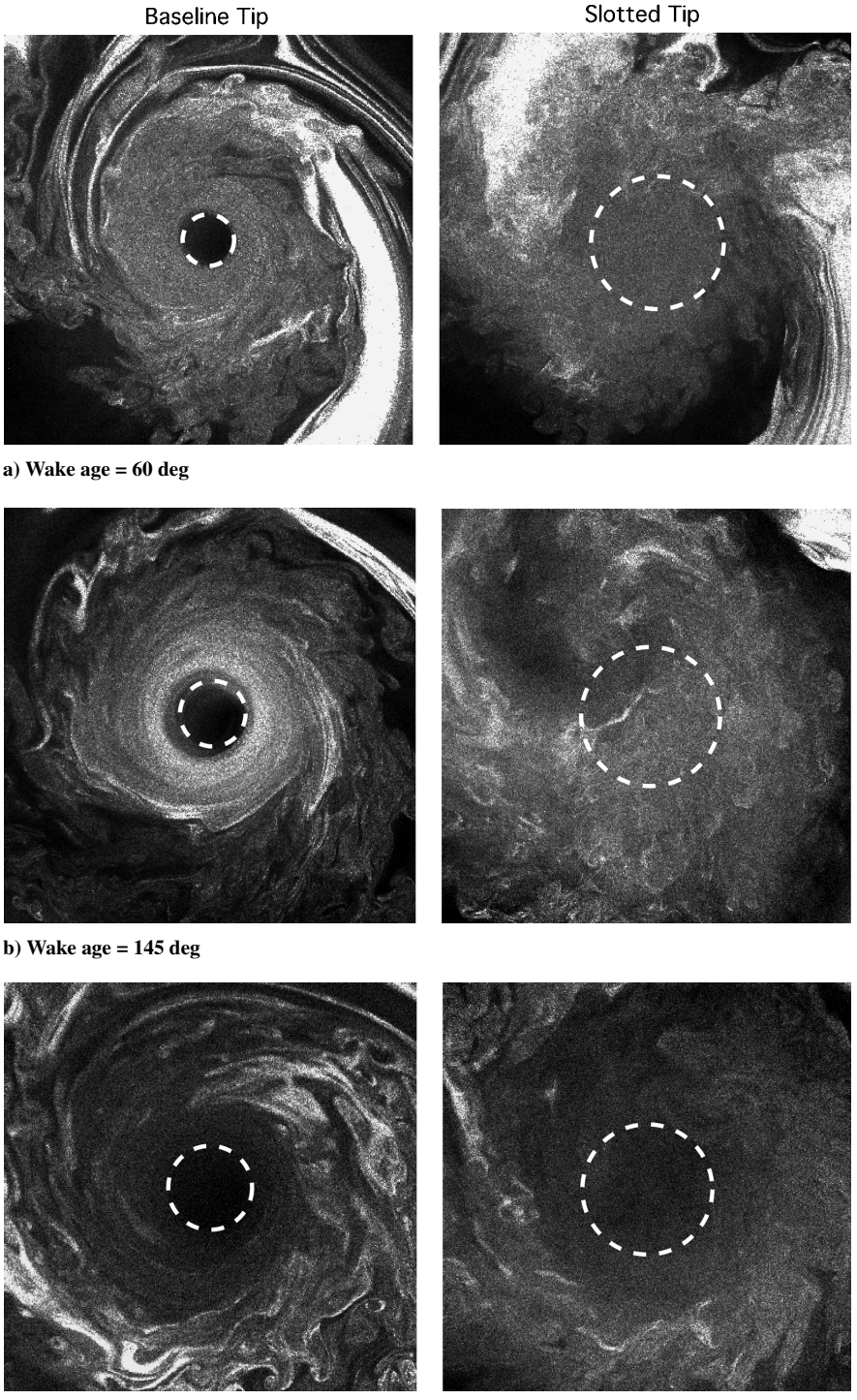

a) Wake age = 60 deg

b) Wake age = 145 deg

c) Wake age = 180 deg

Fig. 9 Close-up of both tip vortex cores with the measured core sizes at comparable wake ages for both blades: – – – circles, measured core size.

In light of these difficulties, the circulation at a specified radial distance from the core is easier to estimate; the results of which are shown in Fig. 12. In this plot, the circulation was estimated at a location equal to six times the core radius. Note that isolated vortex models contain a fixed value of overall circulation strength inside the core. The values typically range from 50% in the case of a Vatistas $n = 1$ profile up to 72% in the case of a Lamb–Oseen profile. The results measured here indicate that the reference value obtained at $r = 6r_c$ can underestimate the net circulation of the tip vortex. Nevertheless, the present results suggest that the circulation values fall within the range defined by the two vortex models. Therefore, while the slotted tip acts to diffuse vorticity away from the tip vortex core, the net circulation about the vortex is essentially conserved.

Rotor Power Consumption

In general, a device to effect changes to the tip vortex of a helicopter rotor blade is accompanied by some power penalty, usually because it significantly increases profile drag.[4,5] This is true even for boundary-layer control devices such as suction or blowing because the technique needs extra power.[11] The addition of subwings, spoilers, or winglets is known to cause a more severe power penalty,[7–9,11] which renders these devices impractical for use on real helicopter rotors. Therefore, for the present slotted tip device it is important to

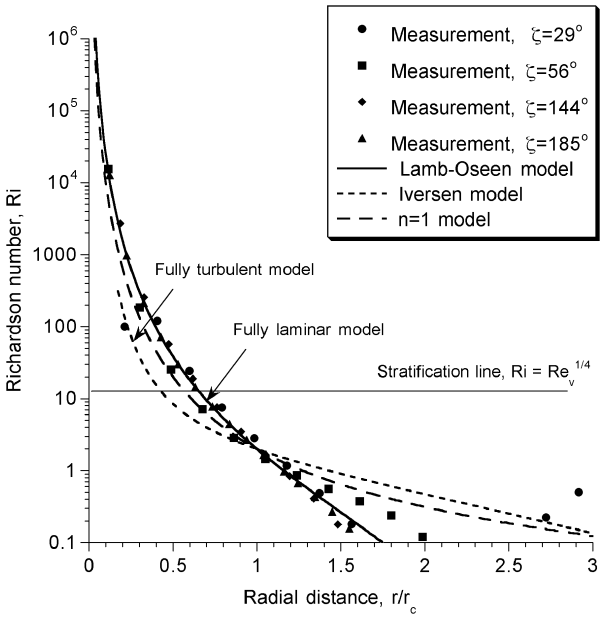

a) Baseline tip

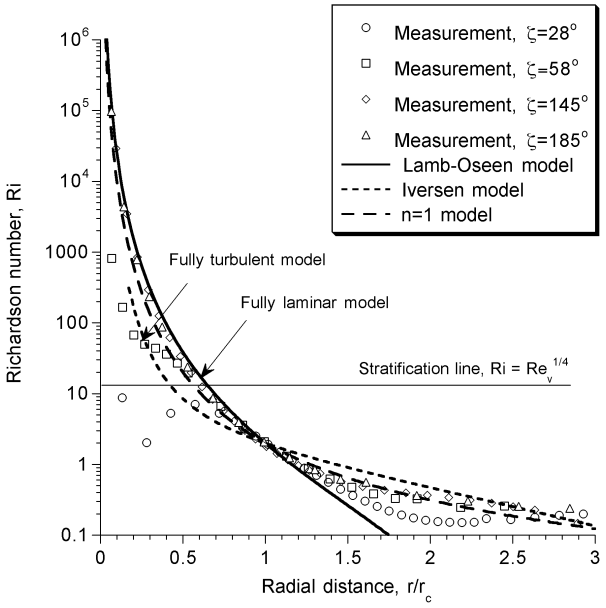

b) Slotted tip

Fig. 10 Distribution of local Richardson number for the baseline blade and the slotted tip blade.

examine the relative power required relative to that of the baseline blade.

For each blade, a direct power measurement was made, which is shown in Fig. 13 as the change in power for the slotted tip rotor relative to the baseline vs the rotational speed. It was found that the slotted tip blade produced a power penalty of less about 4% compared to the baseline blade, which is remarkably low compared to other proposed devices. Of course, compared to the baseline blade, the slotted blade gives a larger wake momentum deficit than the baseline blade, which has been observed in previous experiments.[12,13] Based on the conservation of the kinetic energy of the isolated tip vortex, the axial velocity component increases when the swirl velocity decreases. It can be explained that the slotted blade tends to minimize the momentum loss by confining the turbulent mixing to within the core region of the tip vortex. Any device that attempts to change the vortex by an external action is always accompanied by a substantial momentum loss, which results in much higher performance penalties on a rotor.

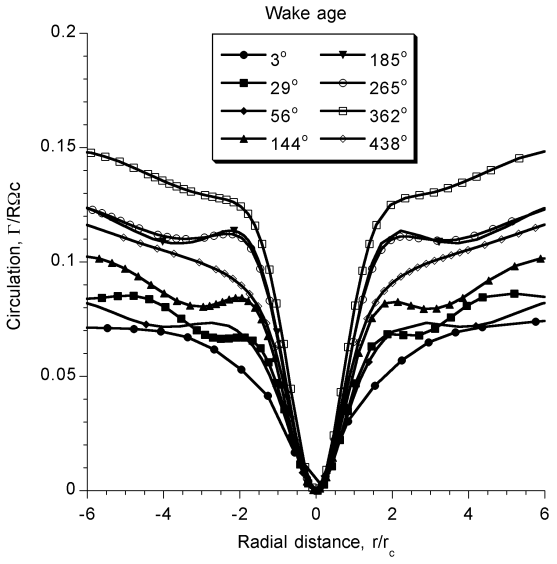

a) Baseline tip

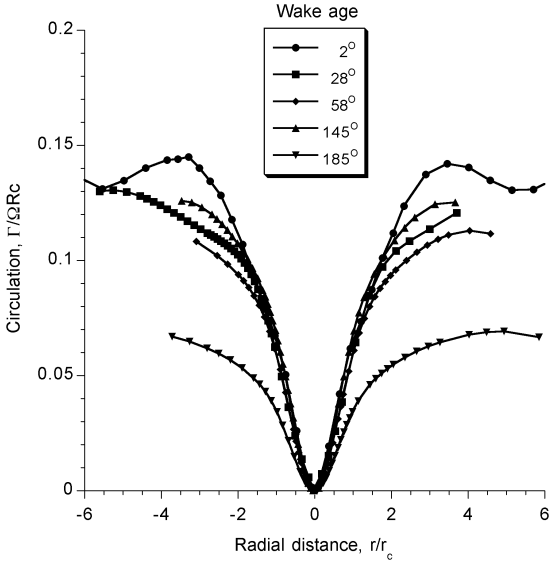

b) Slotted tip

Fig. 11 Distribution of local circulation for the baseline blade and the slotted tip blade.

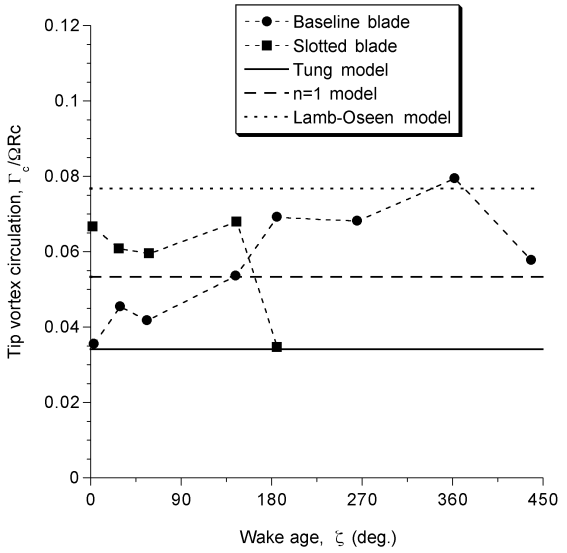

Fig. 12 Core circulation versus wake age for the baseline and slotted blade tips.

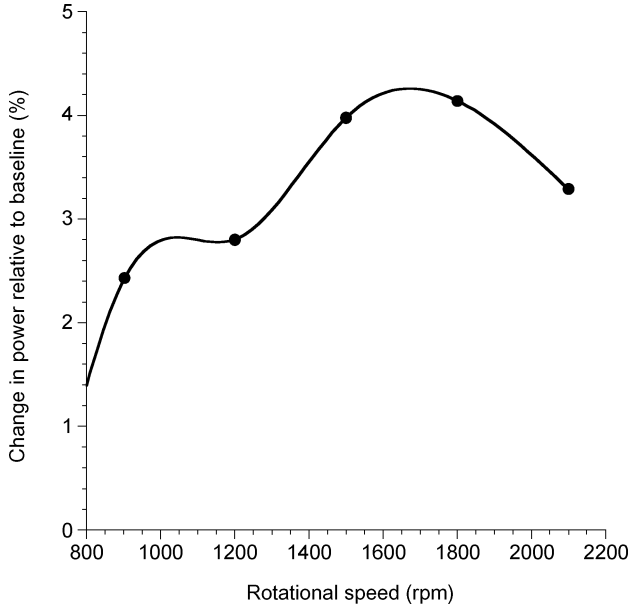

Fig. 13 Relative increase in rotor power requirements for the slotted blade as a function of rotor rpm.

Conclusions

A slotted-tip rotor blade has been designed to rapidly diffuse the vorticity contained within its concentrated tip vortex. The measured results showed that the slotted tip was a highly effective device in accomplishing this goal, which was obtained with only a small rotor power penalty relative to a baseline blade. The slotted blade is, therefore, proposed as a simple, low-cost and highly effective practical device to attenuate and defuse the tip vortex generated by a helicopter rotor. The practical implications for alleviating adverse tip-vortex-induced phenomena on rotorcraft with such a device are enormous, including both rotor noise and overall vibration reductions.

The following conclusions have been drawn from the experimental study:

1) Compared to those of the baseline blade, the peak values of the swirl velocity induced by the tip of the slotted blade were reduced by nearly two-thirds of those found with the baseline, standard rectangular tip. The corresponding core radius was found to be larger by between two to three times when measured at comparable wake ages.

2) Two different mechanisms of vorticity diffusion were observed. The tip vortex of the slotted blade diffuses rapidly because of enhanced flow mixing in the inner core, which prevents a laminar region from being sustained. The tip vortex of the baseline blade diffuses by vortex partitioning (or cascading) at the outer region of the vortex boundary.

3) The slotted blade incurs less than a 3% loss in hovering power compared to that of the baseline blade. This confirms that the present device is much more effective in modifying the internal core structure without penalty than by changing the vortex by the addition of an external device such as a subwing or a spoiler.

Appendix: Aperiodicity Correction

Various methods have been proposed for correcting measurements for aperiodicity or wandering.[32–34] Aperiodicity is the inherent random movement of the phase-resolved spatial locations of the vortex cores inside the rotor wake. Measurements of aperiodicity were made using laser light-sheet illumination of the seeded flow. The laser was synchronized to the rotor so that the aperiodicity of the core position could be measured at a fixed wake age. A CCD camera with a microlens acquired the images, which were digitized and the vortex positions quantified with respect to a calibration grid.

The method of Leishman[33] is used here. Consider the two-dimensional aperiodic motion of a tip vortex at a given wake age ζ. Define the LDV measurement location, which is fixed with respect to the rotor axes system, as (r_p, z_p). The current location of the vortex core axis relative to a rotor based axis system is assumed to be (r_v, z_v). The velocity field measured at (r_p, z_p) at a wake age ζ will be functions of r and z and the position of the measurement point relative to an axis at the center of the vortex, that is,

$$V(r, z, \zeta) = V(r_p - r_v, z_p - z_v, \zeta) \tag{A1}$$

As shown by Devenport et al.,[32] over a sufficiently large number of rotor revolutions the aperiodicity of the vortex location relative to the measurement point can be described by using a probability density function (PDF), say, $p = p(r_v, z_v, \zeta)$ and a joint normal PDF can be defined as

$$p(r_p, z_p, \zeta) = \frac{1}{2\pi\sigma_r\sigma_z\sqrt{1-e^2}} \times \exp\left[\frac{-1}{2(1-e^2)}\left(\frac{r_v^2}{\sigma_r^2} + \frac{z_v^2}{\sigma_z^2} - \frac{2\,e\,r_v z_v}{\sigma_r\sigma_z}\right)\right] \tag{A2}$$

where $\sigma_r = \sigma_r(\zeta)$ and $\sigma_z = \sigma_z(\zeta)$ are the measured rms aperiodicity amplitudes in the radial and axial directions at each wake age, respectively, and $e = e(\zeta)$ is the correlation coefficient. Using Eq. (A2), the actual or measured velocity $\bar{V}(r_p, z_p, \zeta)$ can then be determined numerically by convolution where

$$\bar{V}(r_p, z_p, \zeta) = \int^{\infty}\int_{-\infty} V(r_p - r_v, z_p - z_v, \zeta)\,p(r_v, z_v)\,\mathrm{d}r_v\,\mathrm{d}z_v \tag{A3}$$

which is solved by reexpressing V in a Cartesian coordinate system, and the summations are taken over length scales that are at least one order of magnitude larger than σ. Starting from an initial (assumed) tangential velocity profile without any aperiodicity, a profile with the effects of a measured aperiodicity can be obtained numerically by using Eq. (A3). By comparing this profile to the measured velocity profile, the process proceeds by fixed point iteration. The final result is an estimate of the true velocity field.

Acknowledgments

This work was conducted at the Alfred Gessow Rotorcraft Center at the University of Maryland and was supported by the U.S. Army at NASA Ames Research Center. Additional support was provided by Yeungnam University (YURG2002) and the University of Maryland. Chee Tung was the Technical Monitor. Our appreciation also extends to Yung Yu of the National Rotorcraft Technology Center. Our thanks to Manikandan Ramasamy for his help with the experiments. This paper was presented, in part, at the 59th Annual Forum and Technology Display of the American Helicopter Society International, Phoenix, AZ, 6–8 May 2003.

References

[1]Leishman, J. G., and Bagai, A., "Challenges in Understanding the Vortex Dynamics of Helicopter Rotor Wakes," *AIAA Journal*, Vol. 36, No. 7, 1998, pp. 1130–1140.

[2]Leishman, J. G., *Principles of Helicopter Aerodynamics*, Cambridge Univ. Press, Cambridge, England, U.K., 2000, Chap. 10.

[3]Schmitz, F. H., "Rotor Noise," *Aeroacoustics of Flight Vehicles: Theory and Practice*, Vol. 1, NASA Reference Publication 1258, Aug. 1991, Chap. 2.

[4]Berry, J. D., and Mineck, R. E., "Wind Tunnel Test for an Articulated Helicopter Rotor Model with Several Tip Shapes," NASA-TM-80080, Dec. 1980.

[5]Smith, D. E., and Sigl,. D., "Helicopter Rotor Tip Shapes for Reduced Blade Vortex Interaction—An Experimental Investigation," AIAA Paper 95-0192, Jan. 1995.

[6]Martin, P. B., and Leishman, J. G., "Trailing Vortex Measurements in the Wake of a Hovering Rotor Blade with Various Tip Shapes," *Proceedings of the 58th Annual Forum of the American Helicopter Society International*, American Helicopter Society, Alexandria, VA, 2002.

[7]Tangler, J. L., "Experimental Investigation of the Subwing Tip and Its Vortex Structure," NASA CR-3058, Nov. 1978.

[8]Marchman, J. F., III, and Uzel, J. N., "Effect of Several Wing Tip Modifications on a Trailing Vortex," *Journal of Aircraft*, Vol. 9, No. 9, 1972, pp. 684–686.
[9]McAlister, K. W., Tung, C., and Heineck, J. T., "Devices that Alter the Tip Vortex of a Rotor," NASA TM-2001-209625 (AFDD/TR-01-A-003), Feb. 2001.
[10]Kantha, H. L., Lewellen, W. S., and Durgin, F. H., "Response of a Trailing Vortex to Axial Injection into the Core," *Journal of Aircraft*, Vol. 9, No. 3, 1972, pp. 254–256.
[11]Liu, Z., Russel, J. W., and Sankar, L. N., "A Study of Rotor Tip Structure Alteration Technique," *Journal of Aircraft*, Vol. 38, No. 3, 2001, pp. 473–477.
[12]Han, Y. O., and Bae, H., "Modification of the Tip Vortex by Spanwise Slots," *KSAS Korean Journal*, Vol. 27, No. 5, 1998, pp. 1–7.
[13]Han, Y. O., and Chung, W. J., "Mean and Turbulent Characteristics of Tip Vortices Generated by a Slotted Model Blade," *Proceedings of the 5th Engineering Turbulence Modeling and Measurements*, edited by W. Rodi and N. Fueyo, Vol. 5, Elsevier Science, Oxford, 2002, pp. 637–646.
[14]Martin, P. B., Bhagwat, M. J., and Leishman, J. G., "Strobed Laser-Sheet Visualization of a Helicopter Rotor Wake," *Journal of Flow Visualization and Image Processing*, Vol. 7, No. 1, 2000, pp. 31–50.
[15]Bhagwat, M. J., and Leishman, J. G., "Stability Analysis of Rotor Wakes in Axial Flight," *Journal of the American Helicopter Society*, Vol. 45, No. 3, 2000, pp. 165–178.
[16]Leishman, J. G., "Seed Particle Dynamics in Tip Vortex Flow," *Journal of Aircraft*, Vol. 33, No. 4, 1996, pp. 823–825.
[17]Martin, P. B., Pugliese, G. J., and Leishman, J. G., "Laser Doppler Velocimetry Uncertainty Analysis For Rotor Blade Tip Vortex Measurements," AIAA 2000-0263, Jan. 2000.
[18]Barrett, R. V., and Swales, C., "Realisation of the Full Potential of the Laser Doppler Anemometer in the Analysis of Complex Flows," *Aeronautical Journal*, Vol. 102, No. 10, 1998, pp. 313–320.
[19]Tung, C., Caradonna, F. X., and Morse, H. A., "The Structure of Trailing Vortices Generated by Model Rotor Blades," *Vertica*, Vol. 7, 1983, pp. 33–43.
[20]Tennekes, H., and Lumley, J. L., *A First Course in Turbulence*, MIT Press, Cambridge, MA, 1972, Chap. 1.
[21]Vatistas, G. H., Kozel, V., and Mih, W. C., "Simpler Model for Concentrated Vorticies," *Experiments in Fluids*, Vol. 24, No. 11, 1991, pp. 73–76.
[22]Lamb, H., *Hydrodynamics*, 6th ed., Cambridge Univ. Press, Cambridge, England, U.K., 1932, Chap. 7.
[23]Oseen, C. W., "Uber Wirbelbewegung in Einer Reiben den Flussigkeit," *Archiv fur Matematik und Astronomi och Fysik*, Vol. 7, 1912, pp. 14–21.
[24]Bhagwat, M. J., and Leishman, J. G., "Viscous Vortex Core Models for Free-Vortex Wake Calculations," *Proceedings of the 58th Annual Forum of the American Helicopter Society International*, American Helicopter Society, Alexandria, VA, 2002.
[25]Bhagwat, M. J., and Leishman, J. G., "Correlation of Helicopter Rotor Tip Vortex Measurements," *AIAA Journal*, Vol. 38, No. 2, 2000, pp. 301–308.
[26]Squire, H. B., "The Growth of a Vortex in Turbulent Flow," *Aeronautical Quarterly*, Vol. 16, Aug. 1965, pp. 302–305.
[27]Cotel, A. J., and Breidenthal, R. E., "Turbulence Inside a Vortex," *Physics of Fluids*, Vol. 11, No. 10, 1999, pp. 3026–3029.
[28]Cotel, A. J., "Turbulence Inside a Vortex: Take Two," *Physics of Fluids*, Vol. 14, No. 8, 2002, pp. 2933, 2934.
[29]Bradshaw, P., "The Analogy Between Streamline Curvature and Bouyancy in Turbulent Shear Flows," *Journal of Fluid Mechanics*, Vol. 36, Pt. 1, pp. 177–191.
[30]Iverson, J. D., "Correlation of Turbulent Trailing Vortex Decay Data," *Journal of Aircraft*, Vol. 13, No. 3, 1976, pp. 338–342.
[31]Bhagwat, M. J., and Leishman, J. G., "Measurements of Bound and Wake Circulation on a Helicopter Rotor," *Journal of Aircraft*, Vol. 37, No. 2, 2000, pp. 227–234.
[32]Devenport, W. J., Rife, M. C., Liapis, S. I., and Follin, G. J., "The Structure and Development of a Wing-Tip Vortex," *Journal of Fluid Mechanics*, Vol. 312, 1996, pp. 67–106.
[33]Leishman, J. G., "Measurements of the Aperiodic Wake of a Hovering Rotor," *Experiments in Fluids*, Vol. 25, 1998, pp. 352–361.
[34]Gursul, I., and Xie, W., "Origin of Vortex Wandering over Delta Wings," *Journal of Aircraft*, Vol. 37, No. 2, 1999, pp. 348–350.

R. Lucht
Associate Editor